MR TAGGING FROM A SIGNAL PROCESSING PERSPECTIVE

Ersin Bayram[1], Craig A. Hamilton[1], W. Gregory Hundley[2]

[1]: Medical Engineering Department [2]: Internal Medicine, Cardiology Section
Wake Forest University School of Medicine, NC, USA

Abstract— **Although magnetic resonance (MR) tagging has been shown to be a useful tool in myocardial motion quantification, its clinical utilization is limited as current available methods generally either lack computational speed or require extensive user intervention. Recently, the harmonic phase imaging (HARP) technique has been proposed to look at the phase information of the tagged images [1], [2]. HARP imaging promises to overcome the limitations of existing methods in terms of both computational speed and automation. Motivated by this work, we present mathematical analysis providing a signal processing perspective on the HARP technique. This new perspective provides a clearer understanding of how tags can be accurately tracked using highly-filtered data.**

Keywords— **MR tagging, phase image, myocardial motion, Fourier Spectrum, band-pass filtering, sampling**

I. Introduction

MR tagging is a powerful, non-invasive method to quantify myocardial wall motion and identify abnormalities indicative of regional ischemia. Tags are temporary markers created by spatially encoded saturation planes whose deformations follow the motion in the underlying tissue [3], [4]. After administration of tags with spatially selective rf pulses, the deformation is observed through a sequence of images acquired over the cardiac cycle. Fig.1.(a) is a planar tagged image acquired at end-diastole right after the administration of tags and Fig.1.(b) is acquired near end-systole showing the deformation of tags. Both images have been cropped to display a region of interest (ROI) around the heart for better visualization purposes.

Although creating tagged images is a simple process, extracting the tag deformation within the myocardium is a serious challenge, especially considering the fact that tags are only couple pixels wide. At each image, one has to trace myocardial contours to detect the end points as well as the deformed tags within the myocardium. The complex motion of the heart makes it difficult to utilize a parametric characterization of the tag deformation. Because of short scan times, tagged images are often poor quality, suffering from low signal-to-noise ratio (SNR). Furthermore, T1 recovery of the tagged tissue eliminates the use of simple intensity based methods. Despite all these problems, there are numerous successful approaches in the literature. Tag profile fitting [5] and correlation methods [6] have been successfully implemented. Unfortunately, such methods are computationally intensive, requiring long processing times.

There are several approaches that look into the Fourier content of the tagged images to address the long computation time problem [1], [7]. Especially, the HARP imaging technique appears to be very promising as a clinical tool in terms of speed and minimal user intervention [1], [2]. In HARP imaging, spatial modulation of magnetization (SPAMM) tagging is defined as a modulation process. Hence, the discrete Fourier Transform (DFT) of a tagged image has spectral peaks at integer multiples of the tagging frequency. Bandpass filtering the proper peak results in an image in the spatial domain whose phase values give the tag deformation.

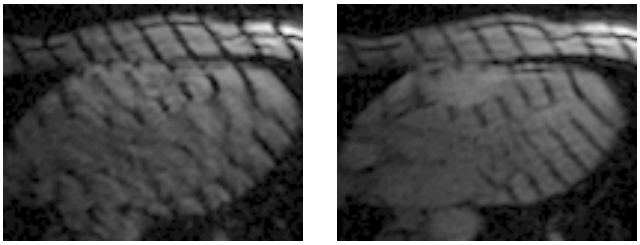

(a) (b)

Fig. 1. Planar tagged image at (a) end-diastole, and (b) end-systole

In this paper, we present a mathematical analysis of the tag deformation from a signal processing perspective, and validate the results of the HARP imaging. Our main contribution to the literature is the introduction of tagging as a sampling process. We believe that analyzing tagging from a signal processing perspective will initiate the introduction of new methods to the tag analysis problem. Furthermore, a mathematical derivation of the phase values for the tag points is given in this work.

II. Methodology

From a signal processing perspective, tagging can be defined as a sampling process such that tagged image is simply the difference of the original image and its sampled version at the tag locations. Hence, the tagged image can be expressed as:

$$o(x,y,t) = u(x,y,t) - u(x,y,t)tag(x,y,t) \qquad (1)$$

where
$o(x,y,t)$: tagged image
$u(x,y,t)$: untagged image
$tag(x,y,t)$: tag pattern

In signal processing, a train of impulse function lines is called the *shah* function ($III(x,y)$). In an $N \times N$ image, the horizontally placed planar tag pattern with a tag separation of $T(t)$ can be represented in terms of shah function as follows:

E.B.: ebayram@wfubmc.edu C.A.H.: crhamilt@wfubmc.edu

Report Documentation Page

Report Date	Report Type	Dates Covered (from... to)
25 Oct 2001	N/A	-

Title and Subtitle MR Tagging From A Signal Processing Perspective	**Contract Number**
	Grant Number
	Program Element Number
Author(s)	**Project Number**
	Task Number
	Work Unit Number
Performing Organization Name(s) and Address(es) Medical Engineering Department Wake Forest University School of Medicine, NC	**Performing Organization Report Number**
Sponsoring/Monitoring Agency Name(s) and Address(es) US Army Research, Development & Standardization Group (UK) PSC 802 Box 15 FPO AE 09499-1500	**Sponsor/Monitor's Acronym(s)**
	Sponsor/Monitor's Report Number(s)

Distribution/Availability Statement
Approved for public release, distribution unlimited

Supplementary Notes
In Supplementary notes put: Papers from 23rd Annual International Conference of the IEEE Engineering in Medicine and Biology Society, October 25-28, 2001, held in Istanbul, Turkey. See also ADM001351 for entire conference on cd-rom.

Abstract

Subject Terms

Report Classification unclassified	**Classification of this page** unclassified
Classification of Abstract unclassified	**Limitation of Abstract** UU

Number of Pages
4

$$tag(x,y,t) = III(\frac{y}{T(t)}) = \sum_{n=0}^{\lfloor \frac{N}{T(t)} \rfloor} \delta(y - nT(t)) \qquad (2)$$

t is the time, x and y are the spatial dimensions satisfying:

$$0 \leq x \leq N-1 \qquad 0 \leq y \leq N-1$$

Tag separation, $T(t)$, is defined as a function of time because its value will change for the non-stationary parts of the tag pattern (i.e. within myocardium). The two dimensional (2D) DFT of Eq.1 in spatial domain gives [8]:

$$O(u,v,t) = U(u,v,t) - \frac{1}{N} U(u,v,t) \otimes_N Tag(u,v,t) \quad (3)$$

where $0 \leq u \leq N-1$ and $0 \leq v \leq N-1$. $\otimes_N$ is the circular convolution operator with period N. The DFT of a shah function is an impulse train (*comb* function) [9]. Hence, $Tag(u,v,t)$ is given by:

$$\begin{aligned} Tag(u,v,t) &= T(t) III\left(\frac{vT(t)}{N}\right)\delta(u) \\ &= T(t) \sum_{k=0}^{\lfloor \frac{N}{T(0)} \rfloor} \delta\left(u, v - k\frac{N}{T(t)}\right) \end{aligned} \qquad (4)$$

From Eq.4 and Eq.3, $O(u,v,t)$ then becomes:

$$O(u,v,t) = U(u,v,t) - \frac{T(t)}{N} \sum_{k=0}^{\lfloor \frac{N}{T(0)} \rfloor} U\left(u, v - k\frac{N}{T(t)}\right) \quad (5)$$

Eq.5 reveals an interesting property of tagged images:

Property 1: *The Fourier spectrum of the tagged image has replications of the untagged image's Fourier spectrum separated by* $\frac{N}{T(t)}$ *pixels from each other.*

It is important to note that although the Fourier spectrum of the tag pattern is a comb function at the time of administration, it's not exactly true for the rest of the frames because of the tag deformation in time. Fortunately, tags do not deform significantly from their initial position, thus their local frequency won't change much. Furthermore, tag pattern is applied to the whole imaging volume. Stationary tags dominates the pattern and forces it to closely follow the behavior of a shah function.

Fig.2.(a) is the natural logarithm of the Fourier spectrum of the image in Fig.1.(b) in which $T(0) = 10$ pixels. The DC component is shifted to the center of the image and natural logarithm is taken to compress the dynamic range for display purposes. The goal is to find $tag(x,y,t)$ and extract the tag deformation. Therefore we are interested in finding $T(t)$. Bandpass filtering the first spectral peak as shown in Fig.2.(a) gives:

$$H(u,v,t) = \begin{cases} \text{O(u,v,t)} & \text{(u,v)} \leq \text{ passband} \\ 0 & \text{elsewhere} \end{cases} \qquad (6)$$

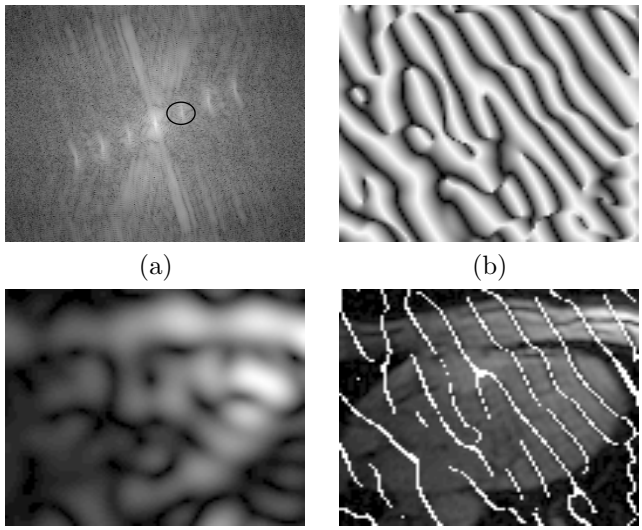

Fig. 2. (a) Fourier spectrum of Fig.1.(a) and the band-pass filter on the first spectral peak. (b) Unwrapped phase magnitude of the IDFT of the first spectral peak in (a). (c) magnitude of the IDFT of the first spectral peak in (a). (d) Detected tag locations

The inverse DFT of $H(u,v,t)$ is a complex image. Applying a circular bandpass filter as in Fig.2.(a) corresponds to convolving the image with a *jinc* function in spatial domain. Hence, the *jinc* function acts as an averaging filter on the image and creates a significant blurring in the magnitude image as shown in Fig.2.(c). $h(x,y,t)$ can be expressed as:

$$h(x,y,t) = -\frac{T(t)}{N} jinc\left(r(T(t)) \otimes_N \left[u(x,y,t) e^{\frac{j2\pi(N)}{NT(t)}y}\right]\right) \qquad (7)$$

with its phase given by:

$$\angle(h(x,y,t) = \frac{2\pi}{T(t)}y + \pi \qquad (8)$$

The π in Eq.(8) comes from the minus sign, as $-1 = e^{j\pi}$. One would expect to have the tag locations close to integer multiples of tagging period $T(t)$. Hence, replacing the y with $kT(t)$, in Eq. 8, the argument of the phase values of tag patterns can be approximated as:

$$\begin{aligned} \arg(\angle(h(x,y,t)) &\approx \left(\frac{2\pi}{T(t)} kT(t) + \pi\right) \bmod (2\pi) \\ &\approx \pi \end{aligned} \qquad (9)$$

The argument of the phase is defined between $[-\pi, \pi)$. Because of the tag deformation and the convolution with the *jinc* function, the argument of the phase values at tag locations might change sign and jump between $-\pi$ and π. The absolute value is taken to solve this problem. Because the spectral peaks on each side of the DC component are anti-symmetric, only one of the first spectral peaks is band-pass filtered to eliminate phase cancellation. Either of the first spectral peaks can be band-pass filtered as the magnitude of the phase information is used. Detected tags are displayed together with the tagged image in Fig.2.(d).

III. Results

A. Computer Simulations

A synthetic image with a tag separation of ten pixels is created. Fig.3.(a) shows the computer generated phantom prior to deformation. Sinusoidal deformations ($\triangle T$) are applied to the image to obtain Fig.3.(b):

$$\triangle T = \frac{T(0)}{2} sin(\phi) \qquad 0 \leq \phi \leq \pi \tag{10}$$

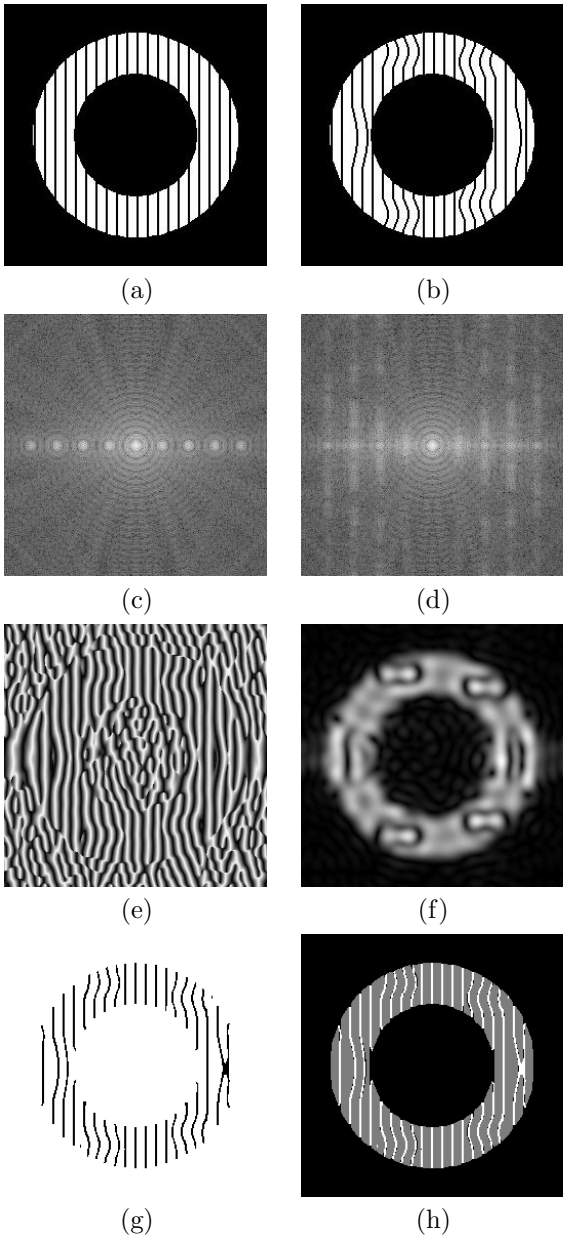

Fig. 3. (a) Non-deformed tag image. (b) Deformed tag image. (c) Fourier spectrum of the non-deformed tag image. (d) Fourier spectrum of the deformed tag image. (e) Unwrapped phase magnitude of the IDFT of the first spectral peak in (d). (f) magnitude of the IDFT of the first spectral peak in (d). (g) Corresponding tag points detected from the phase image. (h) Tagged image and the detected tags added together.

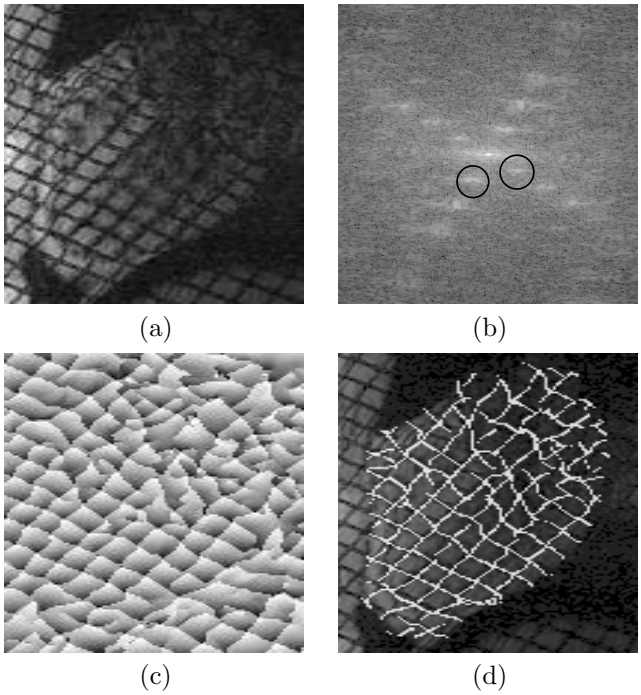

Fig. 4. (a) Grid tagging. (b) Fourier spectrum of the image with the corresponding bandpass filters. (c) Phase images obtained from the inverse Fourier Transform of the bandpass filtered spectral peaks added together (d) Tag locations displayed on top of the heart

Fig.3.(c) and (d) are the corresponding Fourier spectra of these images, respectively. A bandpass filter is applied to the deformed tag spectrum to extract the first spectral peak. The IDFT of this peak is a complex image. The phase map of this complex image is displayed in Fig.3.(e). The agreement between the tag deformation and the phase map can be seen clearly in this image. The magnitude of the IDFT of this peak is shown in Fig.3.(f). As expected from Eq.7, a blur in the magnitude image is observed because of the convolution with the *jinc* function. Morphological closing followed by a simple thresholding is applied to the image in Fig.3.(b) to segment the region of interest and this mask is applied to the tag detected tag points that are extracted from the phase image using a simple thresholding as shown in Fig.3.(g). Detected tag points are added on top of the image in Fig.3.(f) to demonstrate the effectiveness of the method in Fig.3.(h).

B. Grid Tagging

One of the advantages of the method is that it can be easily applied to two dimensional (grid) tagging. Separating the grid type tags into two orthogonal components using the Fourier Spectrum is first proposed by Zhang *et al.* [10]. Mathematically, rotation in spatial domain results in an equivalent rotation in the Fourier domain. Therefore, grid tagging is simply another extra step of 90° rotation plus tagging of the already tagged image. This will create the corresponding spectral peaks in orthogonal directions.

Fig.4.(a) and (b) present a grid tagged image and its corresponding Fourier spectrum, respectively. The user-defined bandpass filters are are also shown for the first

spectral peaks in each tagging direction. Fig.4.(c) shows the resulting phase image by adding the two phase images obtained from the IDFT of the corresponding bandpass filtered spectral peaks. One can see the grid pattern in the phase image indicating the agreement of phase values and the tag deformation. From these two phase images tag patterns are extracted using a simple thresholding around $\frac{\pi}{10}$ neighborhood of π radians. Thresholded images are combined with a logical **OR** operation. Epicardial contour is manually traced in the image and applied as a mask to remove the detected tag patterns outside the region of interest. Resulting image is added on top of the original image as shown in Fig.4.(d) to display the agreement between the detected and actual tag locations.

IV. Discussion

One of the issues in the method is the proper bandpass filter selection. Currently, the user is asked to define the band-pass filter by drawing a circular or polygonal region of interest on the Fourier spectrum of the image. Applying a Gaussian roll off as done in [1] and [7] would reduce the ringing artifact. Another improvement would be automating the filter selection process. A simple thresholding in the Fourier Spectrum image would give us the peak locations and then the bandpass filter can be easily defined without user intervention according to *Property 1*. Currently, the same filter is used for the whole image set. However the DC component of the Fourier spectrum gets larger in time because of the $T1$ recovery of the underlying tagged tissue and might interfere with the band-pass filtered peak. An adaptive scheme can be easily implemented to update the extend of the bandpass filter to eliminate this potential problem. However the drawback of this approach is that reducing the extend of the region also means limiting the ability to detect deformed tags as deformations result in deviations from the center of the band-pass filter region.

Tag tracking is completed under a minute right now including the bandpass filter selection for a set of 30 images with 256×256 dimensions on a Ultra Sparc 400 MHz processor.

The run time would reduce five to ten seconds once the user intervention at the filter selection is eliminated. The algorithm can further be speeded up by parallelizing the process as the tag tracking is performed independently for each frame.

Our emphasis is now on developing a fully automated tag analysis program using this phase information as the tag tracking module.The goal is to complete the myocardial contour segmentation and data analysis under 4 minutes to keep the whole process under 5 minutes to make it useful in clinical setting.

Acknowledgments

The authors would like to thank Mrs. Kimberly Lane for her helpful discussion.

References

[1] N.F. Osman; E.R. McVeigh; J.L. Prince, "Imaging heart motion using harmonic phase mri," *IEEE Transactions on Medical Imaging*, vol. 19, pp. 186–202, 2000.

[2] N.F. Osman; W.S. Kerwin; E.R. McVeigh; J.L. Prince, "Cardiac motion tracking using cine harmonic phase (harp) magnetic resonance imaging," *Magnetic Resonance in Medicine*, vol. 42, pp. 1048–1060, 1999.

[3] E.A. Zerhouni; D.M. Parish; W.J. Rogers; A. Yang; E.P. Shapiro, "Human heart: Tagging with mr imaging-a method for noninvasive assesment of myocardial motion," *Radiaology*, vol. 169, pp. 59–63, 1988.

[4] L. Axel; L. Dougherty, "Mr imaging of motion with spatial modulation of magnetization," *Radiology*, vol. 171, pp. 841–845, 1989.

[5] E. Atalar; E.R. Mcveigh, "Optimization of tag thickness for measuring position with magnetic resonance imaging," *IEEE Transactions on Medical Imaging*, vol. 13, pp. 152–160, 1994.

[6] S.K. Tadikonda; D.J. Fisher; S.M. Collins, "Automated detection of cine-spamm magnetic resonance tags at sub-pixel resolutions," in *Proceedings of Computers in Cardiology*, 1992, pp. 347–350.

[7] S.N. Gupta; J.L. Prince; S.A. Theotokis, "Bandpass optical flow for tagged mr imaging," in *Proceedings of Internatioonal Conference on Image Processing*, 1997, vol. 3, pp. 364–367.

[8] A.V. Oppenheim; R.W. Schafer, *Discrete-Time Signal Processing*, Prentice-Hall, Inc., USA, international edition, 1989.

[9] R.N. Bracewell, *The Fourier Transform and Its Applications*, McGraw-Hill, Inc., USA, second edition, 1986.

[10] S. Zhang; M.A. Douglas; L. Yaroslavsky; R.M. Summers; V. Dilsizan; L. Fananapazir; S. L. Bacharach, "A fourier based algorithm for tracking spamm tags in gated magnetic resonace cardiac images," *Medical Physics*, vol. 23, no. 8, pp. 1359–1369, 1996.